



CrossMark  
click for updates

Cite this: *RSC Adv.*, 2016, 6, 47802

# Dipicolylamine coupled rhodamine dyes: new clefts for highly selective naked eye sensing of Cu<sup>2+</sup> and CN<sup>-</sup> ions†

Kumaresh Ghosh,<sup>\*a</sup> Debojyoti Tarafdar,<sup>a</sup> Anupam Majumdar,<sup>a</sup> Constantin G. Daniliuc,<sup>b</sup> Asmita Samadder<sup>c</sup> and Anisur Rahman Khuda-Bukhsh<sup>c</sup>

The dipicolylamine (DPA) motif which is known as a binder of Zn(II) ions, has been utilized in devising rhodamine labelled compounds **1** and **2**. Compound **1** acts as a FRET sensor and shows excellent selectivity for Cu(II) ions over a series of other cations in CH<sub>3</sub>CN/H<sub>2</sub>O by exhibiting a colour change (colourless to pink) of the solution. The spectral and colour changes are recovered in the presence of CN<sup>-</sup> ions and thus, the ensemble 1·Cu<sup>2+</sup> in CH<sub>3</sub>CN/H<sub>2</sub>O is established as the medium for selective detection of CN<sup>-</sup> ions. In contrast, the modified compound **2** with the dipicolylamine motif as the principal binding site has been established as the colorimetric sensor of Cu(II) ions and the fluorometric sensor of Hg(II), Zn(II) and Cd(II) ions. Both the compounds **1** and **2** are cell permeable and are successfully employed for the detection of intercellular metal ions through bright field and fluorescence imaging.

Received 25th February 2016  
Accepted 2nd May 2016

DOI: 10.1039/c6ra05036k

www.rsc.org/advances

## Introduction

Copper is an essential transition metal ion that plays an important role in environmental, biological and chemical systems.<sup>1</sup> It is toxic to biological systems when the level of Cu<sup>2+</sup> ions exceeds the cellular needs. Overloading of this ion can cause oxidative stress and neurological disorders including Alzheimer's, Parkinson's and Wilson's diseases.<sup>2</sup> Thus rapid sensing of this ion by simple systems is desirable. In this regard, numbers of fluorescent as well as colorimetric sensors for copper ion have been reported in the past few years.<sup>3,4</sup> Of the different chemosensors, rhodamine-labelled sensors draw attention because of visualization of sensing through both color and fluorescence changes.

Rhodamine B and its derivatives exhibit excellent photo-physical properties such as high fluorescence quantum yield, large molar extinction coefficient and visible wavelength excitation. It is further mentionable that the rhodamine B and its derivatives in the spiro-lactam form are non fluorescent (colourless). Upon complexation of metal ions/proton the spiro-lactam ring is opened and shows strong emission as well as

color. Considering this chemistry of rhodamine B, researchers have used this platform in conjunction with different binding sites to construct different metal ion sensors.<sup>5</sup>

Careful scrutiny of the literature reveals that use of dipicolyl amine (DPA) motif as binding site onto the rhodamine unit is less explored in metal ion sensing.<sup>6</sup> Usually this motif binds Zn<sup>2+</sup> ions. The wide spread use of DPA in devising receptors of different architectures for Zn<sup>2+</sup> ion is worth mentioning. Lip-pard *et al.*, have reported dipicolylamine coupled some rhodamine derivatives for sensing of Zn<sup>2+</sup> ions.<sup>6a,b</sup> Not only Zn<sup>2+</sup> ion but also the complexation of Al<sup>3+</sup> and Pb<sup>2+</sup> ions using dipicolyl motif in rhodamine platform is known in few cases.<sup>7</sup> Inspection of such different reports indicates that the disposition of dipicolylamine motif around the rhodamine part is crucial for tuning the metal ion selectivity. In relation to this, design and synthesis of new dipicolylamine coupled rhodamine derivatives thus draws attention.

In this manuscript, we report a new rhodamine-based structure **1** (Fig. 1) that senses Cu<sup>2+</sup> ion through color change involving dipicolyl amine as the binding site. In addition, the ensemble of **1** with Cu<sup>2+</sup> ion is observed to detect CN<sup>-</sup> ion with significant sensitivity. In an effort to understand the role of anthracene in **1** other than FRET, compound **2** was designed and synthesized (Fig. 1). Under identical conditions, compound **2** while selectively senses Cu<sup>2+</sup> ions through color change, it fluorometrically detects some multiple ions such as Hg<sup>2+</sup>, Zn<sup>2+</sup> and Cu<sup>2+</sup> ions without showing any color change. To explain the role of DPA unit in **1** or **2**, the model compound **3** (Fig. 1) was synthesized. Compound **3**, under identical conditions, did not show any selectivity in the recognition process.

<sup>a</sup>Department of Chemistry, University of Kalyani, Kalyani-741235, India. E-mail: ghosh\_k2003@yahoo.co.in; Fax: +913325828282; Tel: +913325828750

<sup>b</sup>Organisch-Chemisches Institut, Universität Münster, Corrensstrasse 40, 48159 Münster, Germany

<sup>c</sup>Department of Zoology, University of Kalyani, Kalyani-741235, India

† Electronic supplementary information (ESI) available: Figures showing the change in fluorescence and UV-vis titrations of **1** and **2** with various cations, packing diagram, Job plots, binding constant and detection limit plots, MTT assay, spectral data. CCDC 1408733. For ESI and crystallographic data in CIF or other electronic format see DOI: 10.1039/c6ra05036k

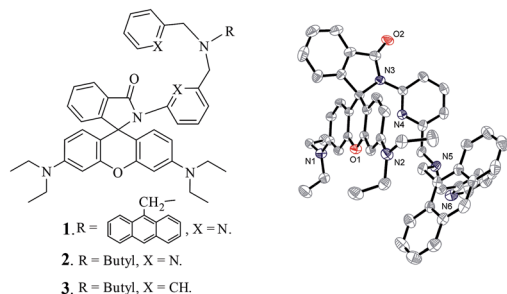
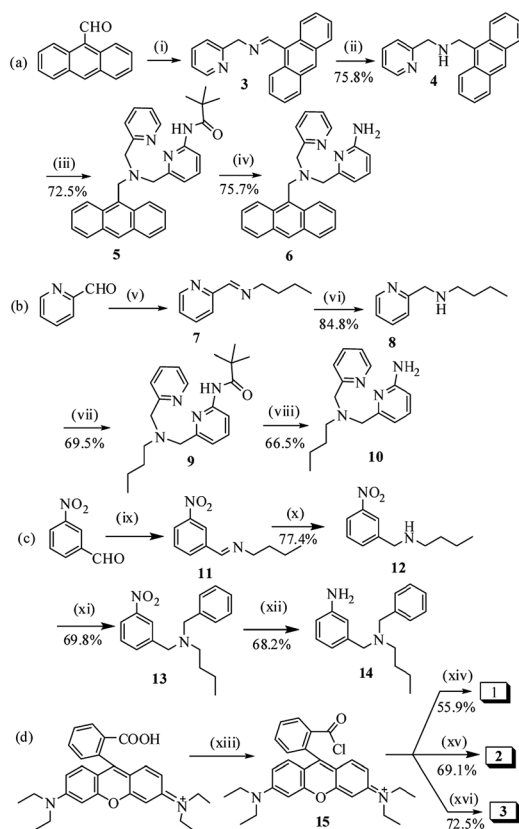


Fig. 1 Chemdraw structures (left) of 1–3 and XP diagram (30% ellipsoids, right) of 1. Hydrogen atoms were omitted for clarity.

## Results and discussion

The synthesis of compound 1 was achieved according to the Scheme 1. Initially, 9-anthraldehyde was transformed into the Schiff base 3 on reaction with 2-picolyamine. Reduction of the Schiff base 3 using  $\text{NaBH}_4$  afforded the amine 4. The amine was



Scheme 1 (a). (i) 2-Picolylamine, dry MeOH, reflux 6 h; (ii)  $\text{NaBH}_4$ , dry MeOH, reflux 6 h; (iii) 2-pivaloylamide-6-bromomethyl pyridine, dry  $\text{K}_2\text{CO}_3$ ,  $\text{CH}_3\text{CN}$ , reflux 8 h; (iv)  $\text{KOH}$ , EtOH, reflux 6 h; (b). (v) *n*-Butylamine, dry MeOH, reflux, 6 h; (vi)  $\text{NaBH}_4$ , dry MeOH, reflux, 6 h; (vii) 2-pivaloylamide-6-bromomethyl pyridine, dry  $\text{K}_2\text{CO}_3$ ,  $\text{CH}_3\text{CN}$ , reflux, 8 h; (viii)  $\text{KOH}$ , EtOH, reflux, 6 h; (c). (ix) *n*-Butylamine, dry  $\text{C}_6\text{H}_6$ , reflux, 6 h, (x)  $\text{NaBH}_4$ , dry MeOH, reflux, 6 h; (xi) benzyl bromide, dry  $\text{K}_2\text{CO}_3$ ,  $\text{CH}_3\text{CN}$ , reflux 6 h; (xii)  $\text{SnCl}_2$ , EtOH, reflux 3 h; (d). (xiii)  $\text{POCl}_3$ , 1,2-dichloroethane, 8 h; (xiv) 6,  $\text{Et}_3\text{N}$ , dry  $\text{CH}_2\text{Cl}_2$ , 6 h; (xv) 10,  $\text{Et}_3\text{N}$ , dry  $\text{CH}_2\text{Cl}_2$ , 6 h; (xvi) 14,  $\text{Et}_3\text{N}$ , dry  $\text{CH}_2\text{Cl}_2$ , 6 h.

reacted with 2-pivaloylamide-6-bromomethyl pyridine which was obtained from 2-amino-6-methylpyridine by reported procedure<sup>8</sup> to obtain the compound 5. Hydrolysis of the amide bond in 5 using  $\text{KOH}$  in EtOH resulted in amine 6 (Scheme 1a). For compound 2, Scheme 1b was pursued to obtain the precursor amine 10 like amine 6. In this case, reaction of pyridine-2-aldehyde with *n*-butylamine in dry MeOH gave Schiff base 7 which on *in situ* reduction with  $\text{NaBH}_4$  yielded amine 8. The amine was reacted with 2-pivaloylamide-6-bromomethyl pyridine to yield the compound 9. Hydrolysis of the amide bond in 9 using  $\text{KOH}$  in EtOH resulted in amine 10 (Scheme 1b). For model compound 3, *m*-nitrobenzaldehyde was converted to the Schiff base 11 which on reduction yielded the amine 12. Benzylation of the amine 12 using benzyl bromide followed by reduction of nitro group furnished the amine 14 in appreciable yield (Scheme 1c). Finally, rhodamine B was converted into its acid chloride 15 with  $\text{POCl}_3$  in 1,2-dichloroethane and was coupled with the amines 6, 10 and 14 to give the desired compounds 1, 2 and 3, respectively in appreciable yields (Scheme 1d). The structures of 1, 2 and 3 were unambiguously characterized by  $^1\text{H}$ ,  $^{13}\text{C}$  NMR and HRMS. For 1, single crystal X-ray analysis further confirmed the structure.

Single crystal of 1 was grown from slow evaporation of acetonitrile solution and was characterized using X-ray crystallography (Fig. 1).<sup>9</sup> In the crystal, compound 1 crystallized in the space group  $P\bar{1}$  and shows the expected orthogonal arrangement of the xanthene unit towards the lactam ring. The angle between the two planes was found to be  $89.8^\circ$ . The nitrogen atom N5 shows sum of the respective C–N–C angles of  $\Sigma\text{N1}^{\text{CCC}} = 332.6^\circ$ . In the packing diagram (see ESI, Fig. 1S†) hydrogen bonding interactions involving the carbonyl group  $\text{C}=\text{O}$  and the C–H units of the diethylamino moieties were found ( $\text{C}-\text{H}\cdots\text{O}$  2.517 Å and 2.761 Å, respectively). Moreover weak  $\pi$ – $\pi$  interactions ( $\sim 3.48$  Å) between two adjacent pyridine groups were detected. No relevant  $\pi$ – $\pi$  interactions involving the anthracene moieties were observed.

The optical responses of compound 1 to various metal cations *viz.*  $\text{Hg}^{2+}$ ,  $\text{Cu}^{2+}$ ,  $\text{Cd}^{2+}$ ,  $\text{Fe}^{2+}$ ,  $\text{Mg}^{2+}$ ,  $\text{Co}^{2+}$ ,  $\text{Ni}^{2+}$ ,  $\text{Zn}^{2+}$ ,  $\text{Ag}^+$ ,  $\text{Fe}^{3+}$ ,  $\text{Mn}^{2+}$ ,  $\text{Na}^+$ ,  $\text{Pd}^{2+}$ ,  $\text{Al}^{3+}$  and  $\text{Pb}^{2+}$  (taken as their perchlorate salts) were investigated in  $\text{CH}_3\text{CN}-\text{H}_2\text{O}$  (4 : 1, v/v, pH = 7.2, 10 mM Tris–HCl buffer) through UV-vis and fluorescence spectroscopic methods. In this context, a high content of water in aqueous measuring solution was desirable, but such an approach was constrained due to the limited solubility of receptor in water. As a reasonable negotiation,  $\text{CH}_3\text{CN} : \text{H}_2\text{O}$  (4 : 1, v/v) was used in the study. It is to note that compound 1 was also found to be soluble in EtOH– $\text{H}_2\text{O}$  (7 : 3, v/v). However, the UV spectrum of 1 in  $\text{CH}_3\text{CN}-\text{H}_2\text{O}$  (4 : 1, v/v, pH = 7.2, 10 mM Tris–HCl buffer) exhibited an intensive band centered at 367 nm which was attributed to the characteristics of anthracene unit. However, addition of  $\text{Cu}^{2+}$  ions produced a new band centered at 552 nm which underwent significant change on progression of titration (Fig. 2). On addition of  $\text{Cu}^{2+}$  ions, the receptor solution became pink in color.

As reason, the appearance of new peak at 552 nm is ascribed to the binding-induced spirolactam ring opening of rhodamine unit in 1. UV-vis titrations of 1 under similar conditions with other metal ions exhibited negligible perturbation in the

spectra showing no peak at 552 nm as well as no color change of the solution (ESI, Fig. 2S†). Thus receptor **1** provides a naked eye detection of  $\text{Cu}^{2+}$  ions among the tested metal ions. Fig. 3 highlights the change in absorbance ratio of **1** and Fig. 4 displays the change in color of the receptor solution in presence of the metal ions examined.

To understand the interference of other metal ions in the sensing of  $\text{Cu}^{2+}$  ion, competition experiment was also carried out by adding  $\text{Cu}^{2+}$  ions to the solutions of **1** in  $\text{CH}_3\text{CN-H}_2\text{O}$  (4 : 1, v/v, pH = 7.2, 10 mM Tris-HCl buffer) in presence of other metal ions (Fig. 5). Results in Fig. 5 indicate that the sensing of  $\text{Cu}^{2+}$  ion by **1** is hardly affected by the ions considered in the study. The sensor **1** shows 1 : 1 stoichiometric interaction (Fig. 6a)<sup>10</sup> with  $\text{Cu}^{2+}$  ion with an association constant<sup>11</sup> value of  $(2.01 \pm 0.28) \times 10^4 \text{ M}^{-1}$  [ $K_d = (4.97 \pm 3.57) \times 10^{-5} \text{ M}$ ] (Fig. 6b). In the sensing of  $\text{Cu}^{2+}$  ions, the detection limit<sup>12</sup> is determined to be  $1.97 \times 10^{-6} \text{ M}$  (ESI, Fig. 3S†).

Compound **1** in  $\text{EtOH-H}_2\text{O}$  (7 : 3, v/v, pH = 7.2, 10 mM Tris-HCl buffer) also exhibited similar results as observed in aq.  $\text{CH}_3\text{CN}$  (ESI, Fig. 4S and 5S†).

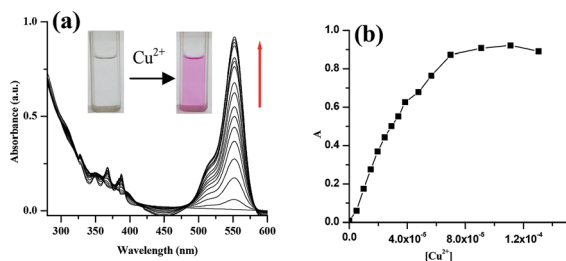


Fig. 2 (a) Change in absorbance of **1** ( $c = 2.5 \times 10^{-5} \text{ M}$ ) in  $\text{CH}_3\text{CN-H}_2\text{O}$  (4 : 1, v/v, pH = 7.2, 10 mM Tris-HCl buffer) upon gradual addition of 2 equiv. amounts of  $\text{Cu}^{2+}$  ( $c = 1 \times 10^{-3} \text{ M}$ ), (b) change in absorption intensity with the addition  $\text{Cu}^{2+}$  ions.

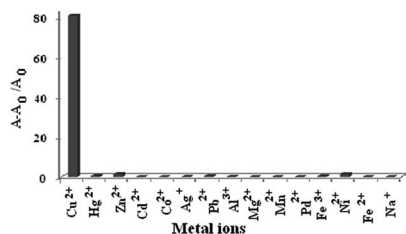


Fig. 3 Change in absorption ratio ( $A - A_0/A_0$ ) of **1** ( $c = 2.5 \times 10^{-5} \text{ M}$ ) at 552 nm upon addition of 2 equiv. amounts of various metal ions in  $\text{CH}_3\text{CN-H}_2\text{O}$  (4 : 1, v/v, pH = 7.2, 10 mM Tris-HCl buffer).



Fig. 4 Photographs showing the color change of the solution of **1** ( $c = 2.5 \times 10^{-5} \text{ M}$ ) in  $\text{CH}_3\text{CN-H}_2\text{O}$  (4 : 1, v/v, pH = 7.2, 10 mM Tris-HCl buffer) in presence of 2 equiv. amounts of metal ions studied.

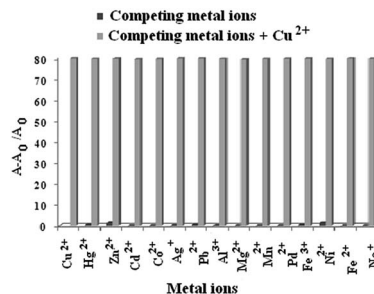


Fig. 5 Competitive selectivity of **1** ( $c = 2.5 \times 10^{-5} \text{ M}$ ) towards  $\text{Cu}^{2+}$  ( $c = 1 \times 10^{-3} \text{ M}$ ) in presence of 2 equiv. of other metal ions in  $\text{CH}_3\text{CN-H}_2\text{O}$  (4 : 1, v/v, pH = 7.2, 10 mM Tris-HCl buffer).

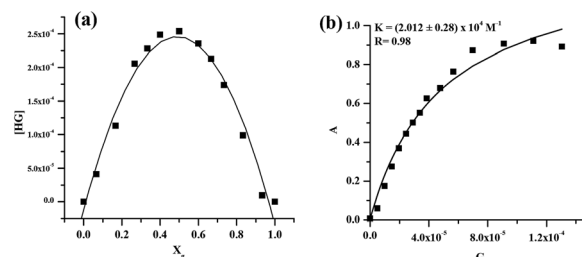


Fig. 6 (a) UV-vis Job plot of receptor **1** with  $\text{Cu}^{2+}$  at 552 nm in  $\text{CH}_3\text{CN-H}_2\text{O}$  (4 : 1, v/v, pH = 7.2, 10 mM Tris-HCl buffer) where  $[\text{H}] = [\text{G}] = 2.5 \times 10^{-5} \text{ M}$ ; (b) binding constant curve from non-linear fitting of UV-vis titration data.

The sensor **1** is a FRET system due to presence of the anthracene at the dipicolyl amine motif. The emission of the intermediate **5** (donor) overlaps with the absorbance of the rhodamine B (acceptor) (Fig. 7a) and thus demonstrates **1** as a FRET system. This FRET-based compound **1** on excitation at the absorbance wavelength 370 nm of anthracene in  $\text{CH}_3\text{CN-H}_2\text{O}$  (4 : 1, v/v, pH = 7.2, 10 mM Tris-HCl buffer) gave structured emission at 416 nm. This emission was due to the anthracene. A broad emission at  $\sim 550 \text{ nm}$  in addition to the monomer emission centered at 416 nm is presumed to be either due to intermolecular excimer between the pyridine rings or due to intermolecular exciplex between anthracene and pyridine. However, upon titration with the metal ions except  $\text{Cu}^{2+}$

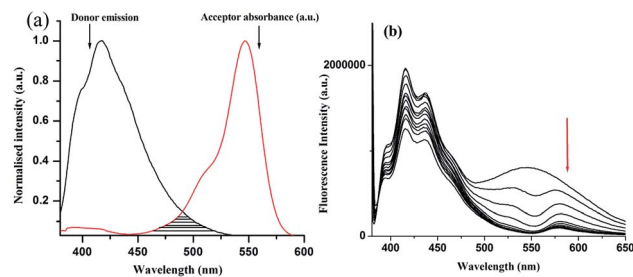
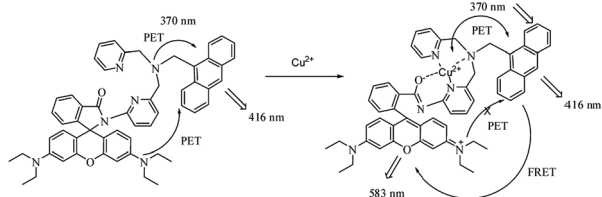


Fig. 7 (a) FRET plot showing the overlapping of emission of donor **5** ( $\lambda_{\text{exc}} = 370 \text{ nm}$ ) and absorbance of acceptor rhodamine B ( $c = 2.5 \times 10^{-5} \text{ M}$ ); (b) change in emission of **1** ( $c = 2.5 \times 10^{-5} \text{ M}$ ) upon gradual addition of 10 equiv. amounts of  $\text{Cu}^{2+}$  ( $c = 1 \times 10^{-3} \text{ M}$ ) in  $\text{CH}_3\text{CN-H}_2\text{O}$  (4 : 1, v/v, pH = 7.2, 10 mM Tris-HCl buffer) ( $\lambda_{\text{exc}} = 370 \text{ nm}$ ).

the intensity of broad emission at  $\sim 550$  nm was reduced showing no splitting in the region 575 nm to 590 nm due to lactam ring opening of rhodamine part (ESI, Fig. 6S<sup>†</sup>). Under this condition, the FRET process remained off. In contrast, in presence of  $\text{Cu}^{2+}$  ions, the broad peak at 550 nm was split into two peaks of which the peak at  $\sim 580$  nm was due to lactam ring opening that activated the FRET process and gave sharp color change (Fig. 7b). However, the intensity of this peak was gradually reduced along with the emission of anthracene at 416 nm on progression of titration and no ratiometric behavior in the emission spectra was observed. This is believed to be due to paramagnetic effect of  $\text{Cu}^{2+}$  ion.<sup>13</sup> Quenching of fluorescence occurs due to the excitation energy transfer from the ligand to the metal d-orbital and/or ligand to metal charge transfer (LMCT) in aqueous  $\text{CH}_3\text{CN}$ .<sup>14</sup> This is in accordance with the observations of other researchers.<sup>14</sup> The peak at 530 nm arising from splitting was finally abolished on progression of titration. Importantly, the compound **1** is a system where the sensing mechanism is an integration of PET (photoinduced electron transfer) and FRET processes (Scheme 2).<sup>15</sup> At pH 7.2, the nitrogen atom of aromatic imino in rhodamine part as well as nitrogen atom of the tripodal centre quench the emission of anthracene to a certain extent. Upon complexation of  $\text{Cu}^{2+}$  ion at the DPA moiety involving the lactam part of rhodamine, the FRET process from anthracene to rhodamine moiety occurs. At the same time, the PET process occurring in between the copper complexed site and the excited state of anthracene remains activated that led to a non ratiometric change in the emission spectrum. This was realized from the recording of the emission spectra of **1** at different pHs.

In Fig. 7b, the appearance of the peak at 580 nm under the broad emission at  $\sim 550$  nm due to  $\text{Cu}^{2+}$ -induced lactam ring opening was confirmed by recording the fluorescence spectra of **1** in presence of acid where  $\text{H}^+$ -induced lactam ring opening in rhodamine system is usual. In this regard, the fluorescence spectra of **1** were recorded at different pHs. As can be seen from Fig. 8a, the sharp peak at 583 nm in fluorescence with considerable intensity was observed from pH 3 to pH 2. Fig. 8b demonstrates that ratio of intensities at 583 nm and 416 nm ( $I_{583}/I_{416}$ ) increases with decrease in pH from 4.00 to 2.00. This observation clearly indicates that anthracene acts as FRET donor in receptor **1** and the receptor **1** behaves as an ideal ratiometric sensing platform at strong acidic condition. It is to note that in pH range 4–12, there was no peak at 583 nm for ring opening (ESI, Fig. 7S<sup>†</sup>). The UV-vis titration spectra with change in pH can be found in the ESI<sup>†</sup> where the absorbance of **1** at 551 nm at pHs 2 and 3 is in conformity with the opening of lactam



Scheme 2 Proposed PET and FRET processes in **1**.

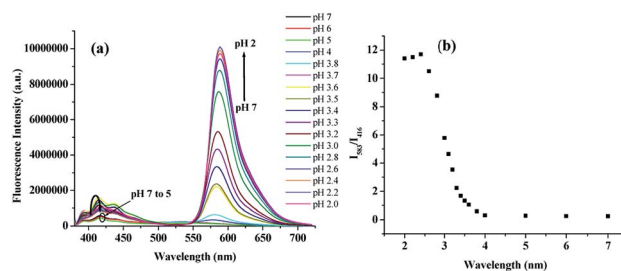


Fig. 8 (a) Fluorescence spectra of **1** ( $c = 2.5 \times 10^{-5}$  M) in  $\text{CH}_3\text{CN}-\text{H}_2\text{O}$  (4 : 1, v/v, 10 mM Tris-HCl buffer) at different pH values ( $\lambda_{\text{exc}} = 370$  nm); (b) change of fluorescence emission ratios ( $I_{583}/I_{416}$ ) by pH values.

ring that resulted in pink color (ESI, Fig. 7S<sup>†</sup>). Interestingly, a similar pH-response of **1** was observed in  $\text{EtOH}-\text{H}_2\text{O}$  (7 : 3, v/v, 10 mM Tris-HCl buffer) (ESI, Fig. 8S<sup>†</sup>).

Thus the selective response of **1** toward  $\text{Cu}^{2+}$  ion in both UV and fluorescence at pH 7.2 is attributed to the coordination of  $\text{Cu}^{2+}$  ion at the dipicolyl moiety involving the lactam part. FTIR spectral analysis of **1** itself and with  $\text{Cu}(\text{ClO}_4)_2$  reveals a shifting of carbonyl stretching frequency from  $1700 \text{ cm}^{-1}$  to  $1650 \text{ cm}^{-1}$  (ESI, Fig. 9S<sup>†</sup>). This indicates the participation of the amide carbonyl in complexation. In order to realize the participation of the pyridine rings in complexation, we tried to record the  $^1\text{H}$  NMR of **1** itself and in presence of 1 equiv. amount of  $\text{Cu}(\text{ClO}_4)_2$  in  $\text{CD}_3\text{CN}/\text{D}_2\text{O}$  (4/1, v/v). Unfortunately, in presence of  $\text{Cu}^{2+}$  the sharp signals for different protons of **1** became too broad to interpret. Then we performed the  $^1\text{H}$  NMR titration of **1** with  $\text{Cu}^{2+}$  ion in pure  $\text{CD}_3\text{CN}$  solvent. In this solvent system, on progression of titration, signals for the three methylenes (types 'a', 'b' and 'c') around the picolyl motif exhibited downfield shifts of 0.07 ppm upon complexation of equivalent amount of  $\text{Cu}^{2+}$  ion. The signals for pyridyl ring protons became broad and underwent small downfield chemical shifts (ESI, Fig. 10S<sup>†</sup>). Addition of more than 2 equiv. amounts of  $\text{Cu}^{2+}$  ions caused broadening of the signals and limits the titration to continue.

This corroborated a weak ground state interaction of **1** with  $\text{Cu}^{2+}$  ion at the DPA moiety in the suggested mode shown in Fig. 9a. To be confirmed with the binding role of pyridyl ring nitrogens in **1**, compound **3** which lacks of pyridine rings was further explored in binding study. In fluorescence and UV-vis titrations, compound **3** exhibited color change in presence of multiple metal ions (e.g.,  $\text{Cu}^{2+}$ ,  $\text{Hg}^{2+}$ ,  $\text{Fe}^{3+}$  and  $\text{Al}^{3+}$ ) in  $\text{CH}_3\text{CN}-$

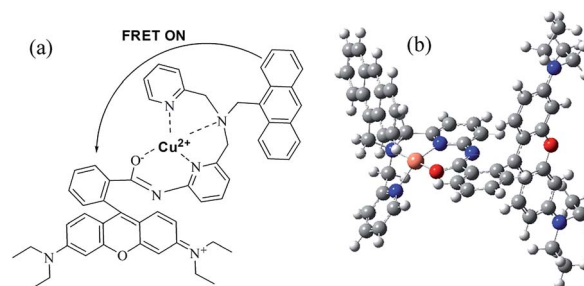


Fig. 9 (a) Suggested binding mode of **1** with  $\text{Cu}^{2+}$  ion; (b) DFT optimized geometry of the complex **1**- $\text{Cu}^{2+}$  in gas phase.

H<sub>2</sub>O (4 : 1, v/v, pH = 7.2, 10 mM Tris-HCl buffer) giving no selectivity in the sensing process (ESI, Fig. 11S and 12S†).

DFT optimization of the copper complex in gas phase (Fig. 9b) reveals that the pyridyl ring nitrogens along with the lactam amide oxygen are intimately involved in coordination of Cu<sup>2+</sup> ion. It is important to be pointed out that the DPA unit which is usually the binder of Zn<sup>2+</sup> ion, prefers the binding of Cu<sup>2+</sup> ion in **1**. We believe that this occurs due to the change in metal coordination environment around the dipicolyl motif. To realize this, we considered the intermediate compound **5** which in fluorescence clearly showed the preference for Zn<sup>2+</sup> and Cd<sup>2+</sup> ions (Fig. 10) like other systems reported in the literature.<sup>16</sup>

Careful scrutiny of the literature reveals that rhodamine coupled with 2-aminopyridine<sup>17a</sup> shows responses towards Fe<sup>3+</sup>, Hg<sup>2+</sup> and Pb<sup>2+</sup> ions instead of Cu<sup>2+</sup>. On the other hand, the dipicolylamine motif in 1,8-naphthalimide system as reported by Yoon *et al.*, is observed to bind Cu<sup>2+</sup> ion instead of Zn<sup>2+</sup> ion.<sup>17b</sup> In addition, rhodamine-coupled 1,2,3-triazole functionalized 2-amino pyridine exhibits selective response to Zn<sup>2+</sup> ions although there was no dipicolyl amine motif in the structure.<sup>17c</sup> These observations thus validate the fact that the selection of a particular metal ion in a binding site is dependent on the coordination environments that regulate the binding of Cu<sup>2+</sup> ions in present example.

In the selective binding of Cu<sup>2+</sup> ion, the effect of the counter anions of different copper salts was observed to be negligible. This can be realized from Fig. 13Sa and b†. Furthermore, the reversibility of the binding process between **1** and Cu<sup>2+</sup> was established by adding aqueous solution of Na<sub>2</sub>EDTA to the solution of **1**·Cu<sup>2+</sup> in both CH<sub>3</sub>CN/aqueous Tris-HCl buffer (4 : 1, v/v, pH = 7.2) and EtOH/aqueous Tris-HCl buffer (7 : 3, v/v, pH = 7.2) solvent systems. In the event, EDTA<sup>2-</sup> caused demetalation of **1** and regeneration of the spirolactam ring with bleaching of absorption band at ~552 nm (ESI, Fig. 13Sc and d†).

As practical application, the copper ion ensemble of **1** was explored in studying the interaction of different anions *viz.* F<sup>-</sup>, Cl<sup>-</sup>, Br<sup>-</sup>, I<sup>-</sup>, NO<sub>3</sub><sup>-</sup>, CN<sup>-</sup>, AcO<sup>-</sup>, ClO<sub>4</sub><sup>-</sup>, HSO<sub>4</sub><sup>-</sup>, HP<sub>2</sub>O<sub>7</sub><sup>3-</sup>, H<sub>2</sub>PO<sub>4</sub><sup>-</sup> (counter cations: Bu<sub>4</sub>N<sup>+</sup>), ATP, ADP, AMP, HPO<sub>4</sub><sup>2-</sup>, PO<sub>4</sub><sup>3-</sup> and P<sub>2</sub>O<sub>7</sub><sup>4-</sup> (counter cations: Na<sup>+</sup>). The addition of different anions to the ensemble perturbed the emission to the different extents (Fig. 11a). Among the anions studied, only CN<sup>-</sup>

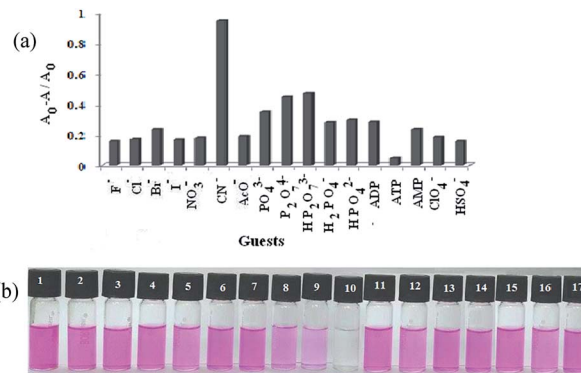


Fig. 11 (a) Change in absorbance ratio at 552 nm for **1**·Cu<sup>2+</sup> ensemble upon addition of 12 equiv. of various anions ( $c = 1 \times 10^{-3}$  M) in CH<sub>3</sub>CN-H<sub>2</sub>O (4 : 1, v/v, pH = 7.2, 10 mM Tris-HCl buffer); (b) photographs showing the color change of the solution of **1** ( $c = 2.5 \times 10^{-5}$  M) in CH<sub>3</sub>CN-H<sub>2</sub>O (4 : 1, v/v, pH = 7.2, 10 mM Tris-HCl buffer) in presence of 12 equiv. of (1) F<sup>-</sup>, (2) Cl<sup>-</sup>, (3) Br<sup>-</sup>, (4) I<sup>-</sup>, (5) NO<sub>3</sub><sup>-</sup>, (6) AcO<sup>-</sup>, (7) ClO<sub>4</sub><sup>-</sup>, (8) P<sub>2</sub>O<sub>7</sub><sup>4-</sup>, (9) HP<sub>2</sub>O<sub>7</sub><sup>3-</sup>, (10) CN<sup>-</sup>, (11) ATP, (12) ADP, (13) AMP, (14) H<sub>2</sub>PO<sub>4</sub><sup>-</sup>, (15) HPO<sub>4</sub><sup>2-</sup>, (16) PO<sub>4</sub><sup>3-</sup>, (17) HSO<sub>4</sub><sup>-</sup>.

ion interacted strongly showing a sharp color change (pink to colorless) and recovery of the original absorbance characteristics of **1**. This also indicated the reversibility in the binding of Cu<sup>2+</sup> ion. In the event, pyrophosphate (P<sub>2</sub>O<sub>7</sub><sup>4-</sup>) responded moderately. The CN<sup>-</sup>- induced color change from pink to colorless solution associated with complete decrease in absorbance at 552 nm of **1**·Cu<sup>2+</sup> complex with 1 : 1 stoichiometric composition suggested that Cu<sup>2+</sup> ion was removed from the binding centre through its complexation with CN<sup>-</sup> ion (Fig. 12a). However, the other tested anions were silent in the process (ESI, Fig. 14S†). Thus, **1**·Cu<sup>2+</sup> complex can be used as a potential ensemble for selective colorimetric naked eye sensing of CN<sup>-</sup> over the other tested anions (Fig. 11b).

It is important to be mentioned that the ensembles prepared from the mixing of **1** with more than 1 equiv. amount of Cu<sup>2+</sup> responded to CN<sup>-</sup> ion in a similar way to that of the ensemble **1**·Cu<sup>2+</sup> having 1 : 1 equiv. combination. Only there was a slight variation in detection limit of CN<sup>-</sup> ion and this is due to minor interference of the free Cu<sup>2+</sup> ion in the ensemble (Fig. 12b).

Considering the interaction of CN<sup>-</sup> ion with the copper ensemble of **1**, a logic operation was performed. Herein, the

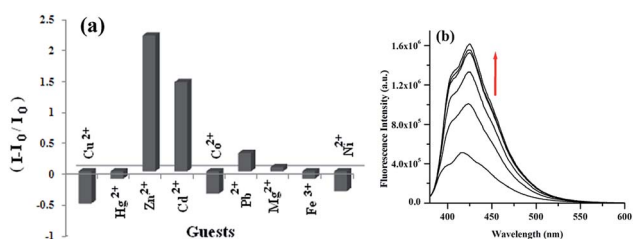


Fig. 10 (a) Change in emission ratio ( $I - I_0/I_0$ ) of **5** ( $c = 2.5 \times 10^{-5}$  M) at 424 nm upon addition of 2 equiv. amounts of various metal ions in CH<sub>3</sub>CN-H<sub>2</sub>O (4 : 1, v/v, pH = 7.2, 10 mM Tris-HCl buffer); (b) change in emission of **5** ( $c = 2.5 \times 10^{-5}$  M) upon gradual addition of 2 equiv. amounts of Zn<sup>2+</sup> ( $c = 1 \times 10^{-3}$  M) in CH<sub>3</sub>CN-H<sub>2</sub>O (4 : 1, v/v, pH = 7.2, 10 mM Tris-HCl buffer) ( $\lambda_{\text{exc}} = 370$  nm).

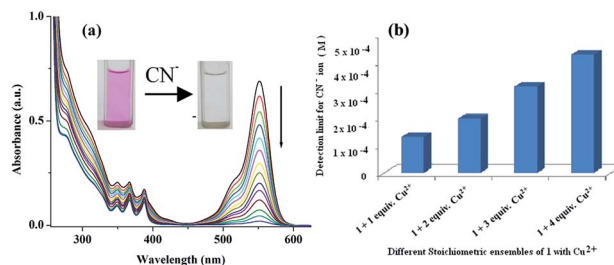


Fig. 12 (a) Emission spectra for **1**·Cu<sup>2+</sup> (**1** : Cu<sup>2+</sup> = 1 : 1 equiv.) ensemble upon gradual addition of 10 equiv. amounts of CN<sup>-</sup> in CH<sub>3</sub>CN-H<sub>2</sub>O (4 : 1, v/v, pH = 7.2, 10 mM Tris-HCl buffer); (b) change in detection limit of CN<sup>-</sup> ion for different stoichiometric ensembles of **1**·Cu<sup>2+</sup>.

sequence dependant “off-on-off” switching of absorption was used to construct a INHIBIT logic gate using  $\text{Cu}^{2+}$  and  $\text{CN}^-$  as chemical inputs. In considering the INHIBIT logic gate properties of **1**,  $\text{Cu}^{2+}$  and  $\text{CN}^-$  ions act as inputs while the absorbance at 552 nm ( $A_{552}$ ) functions as output (Fig. 13a and b). The output is *zero* when (i) both the  $\text{Cu}^{2+}$  and  $\text{CN}^-$  are absent; (ii)  $\text{CN}^-$  alone is present, or (iii) both  $\text{Cu}^{2+}$  and  $\text{CN}^-$  are present, and the gate is OFF. The output is *one* only when  $\text{Cu}^{2+}$  alone is present and the gate is ON. Thus **1** can be used to construct a logic circuit mimicking an INHIBIT gate.

In order to understand the role of anthracene (other than FRET process) in the binding event, compound **2** was next explored in the study. The free receptor **2** ( $c = 3.72 \times 10^{-5}$  M) in  $\text{CH}_3\text{CN}-\text{H}_2\text{O}$  (4 : 1, v/v, pH = 7.2, 10 mM Tris-HCl buffer) exhibited almost negligible absorption peak at 554 nm. However, gradual addition of  $\text{Cu}^{2+}$  ion resulted in a significant enhancement of absorption centered at 554 nm and exhibited a sharp color change from colorless to pink (ESI, Fig. 15S<sup>†</sup>). Such increase in absorbance at 554 nm along with the color change is due to  $\text{Cu}^{2+}$ -induced spiro lactam ring of rhodamine B like the case of **1**. The other tested metal ions did not perturb the absorption spectra of **2** and no color change was noticed. The bar plot in Fig. 15S<sup>†</sup> demonstrates the change in absorption ratio of **2** in presence of 2 equiv. amounts of different metal ions. Thus the binding study clearly reveals that the dipicolylamine motif either in **1** or **2** is sensible to  $\text{Cu}^{2+}$  ion.

Like **1**, the competitive experiment as shown in Fig. 16Sa,<sup>†</sup> suggests that **2** is also able to selectively recognize  $\text{Cu}^{2+}$  in presence of other metal ions. The 1 : 1 stoichiometry of the complex was evaluated from the Job plot<sup>10</sup> using absorbance data (ESI, Fig. 16Sb<sup>†</sup>). The association constant<sup>11</sup> of  $2 \cdot \text{Cu}^{2+}$ , derived from nonlinear curve fitting, was calculated to be  $(4.44 \pm 0.14) \times 10^4 \text{ M}^{-1}$  [ $K_d = (2.23 \pm 7.14) \times 10^{-5} \text{ M}$ ] (ESI, Fig. 17S<sup>†</sup>). The detection limit<sup>12</sup> for **2** towards  $\text{Cu}^{2+}$  ion was found to be  $8.45 \times 10^{-7} \text{ M}$  which is fairly good than the receptor **1** (ESI, Fig. 18S<sup>†</sup>).

Fluorescence titration experiments were performed to gain an insight into the binding interaction of **2** in the excited state. Sensor **2** ( $c = 3.72 \times 10^{-5}$  M) in  $\text{CH}_3\text{CN}-\text{H}_2\text{O}$  (4 : 1, v/v, pH = 7.2, 10 mM Tris-HCl buffer), on excitation at 500 nm, displayed a weak emission at 577 nm. On gradual addition of  $\text{Cu}^{2+}$ ,  $\text{Hg}^{2+}$ ,  $\text{Zn}^{2+}$  and  $\text{Cd}^{2+}$ , significant enhancements in emission of **2** were observed (Fig. 14). Interestingly, in case of addition of  $\text{Cu}^{2+}$ , an

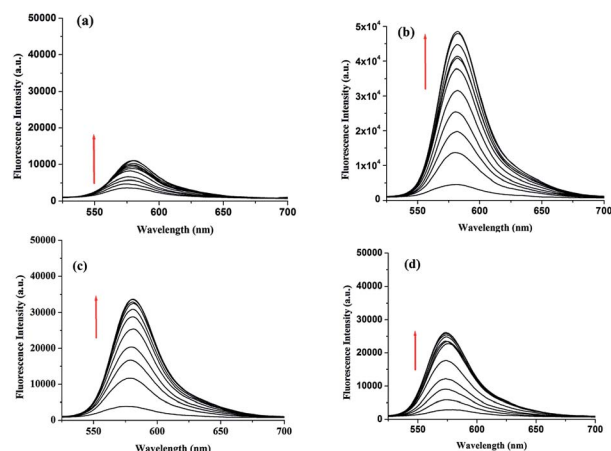


Fig. 14 Change in emission of **2** ( $c = 2.5 \times 10^{-5}$  M) in  $\text{CH}_3\text{CN}-\text{H}_2\text{O}$  (4 : 1, v/v, pH = 7.2, 10 mM Tris-HCl buffer) upon addition of 10 equiv. of (a)  $\text{Cu}(\text{ClO}_4)_2$ , (b)  $\text{Hg}(\text{ClO}_4)_2$ , (c)  $\text{Cd}(\text{ClO}_4)_2$ , (d)  $\text{Zn}(\text{ClO}_4)_2$ . [concentration of metal salts were  $1 \times 10^{-3}$  M] ( $\lambda_{\text{exc}} = 500 \text{ nm}$ ).

increase in emission centered at 577 nm with concomitant color change of the solution from colorless to pink was observed. This suggested the chelation of  $\text{Cu}^{2+}$  ion at the DPA motif involving the amide ion of the spiro lactam ring like the mode shown in Fig. 9a. Interestingly, in presence of  $\text{Hg}^{2+}$ ,  $\text{Zn}^{2+}$  and  $\text{Cd}^{2+}$  ions no color change of the receptor solution was observed. This indicated the intactness of the spiro lactam ring during complexation and the increase in emission in such cases is attributed to the complexation of metal ions into the dipicolyl core leading to inhibition of PET process occurring in between the binding site and the excited state of rhodamine. The increment in emission intensity of **2** was significantly higher with the addition of  $\text{Hg}^{2+}$  ion (ESI, Fig. 19S<sup>†</sup>).

However, excitation of **2** in fluorescence at 370 nm instead of 500 nm gave emission at  $\sim 450 \text{ nm}$  (presumably for the DPA motif) which underwent small increase in presence of  $\text{Hg}^{2+}$ ,  $\text{Zn}^{2+}$  and  $\text{Cd}^{2+}$  ions showing no color change (lactam ring intact) in the solution. Under the similar conditions, mere change in emission of **2** at 450 nm with a color change (opening of lactam ring) upon gradual addition of  $\text{Cu}^{2+}$  ions was due to paramagnetic effect of  $\text{Cu}^{2+}$  ion<sup>13</sup> that quenched the emission (ESI, Fig. 20S<sup>†</sup>). This control experiment highlighted the key role of anthracene in **1** as FRET donor in the selective sensing of  $\text{Cu}^{2+}$  ions.

Like **1**, receptor **2** was pH sensitive; the color change from colorless to pink was only observed at pHs 2 and 3 (ESI, Fig. 21S<sup>†</sup>). Receptor **2** was further explored in anion sensing through the use of its copper ensemble like **1**. Among the various anions as considered in case of **1**, only  $\text{CN}^-$  affected the spectral pattern of the ensemble  $2 \cdot \text{Cu}^{2+}$ , exhibiting a significant decrease in absorbance (ESI, Fig. 22Sa<sup>†</sup>). Cyanide ion-induced decrease in absorption of the ensemble  $2 \cdot \text{Cu}^{2+}$  resulted in a sharp color change from pink to colorless. Other tested anions perturbed the absorption of the ensemble to the negligible extents (ESI, Fig. 22Sb<sup>†</sup>). Like **1**, the ensembles prepared from mixing of **2** with **1** or more than 1 equiv. amounts of  $\text{Cu}^{2+}$  were sensitive to  $\text{CN}^-$  ion and gave a slight variation in detection

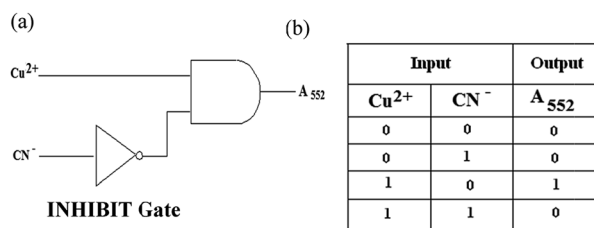


Fig. 13 (a) Logic circuit of receptor **1** with  $\text{Cu}^{2+}$  and  $\text{CN}^-$  as chemical inputs and  $A_{552}$  as output of the INHIBIT gate, (b) truth table for the INHIBIT gate of **1** with  $\text{Cu}^{2+}$  and  $\text{CN}^-$  as chemical inputs and  $A_{552}$  as output.

limit of  $\text{CN}^-$  ion for minor interference of the free  $\text{Cu}^{2+}$  ion in the ensembles (ESI, Fig. 23S†).

Thus the experimental findings on structure **2** demonstrate that the replacement of anthracene part in **1** has a marked effect in sensing process. The anthracene part in **1** exerts a steric environment for which the dipicolylamine motif only allows the  $\text{Cu}^{2+}$  ion in the interaction process. In contrast, the butyl chain in **2** being less steric allows not only  $\text{Cu}^{2+}$  ion but also other ions such as  $\text{Zn}^{2+}$ ,  $\text{Cd}^{2+}$  and  $\text{Hg}^{2+}$  ions although the binding mechanism is different.

The potentiality of **1** and **2** in biological systems was evaluated for *in vitro* detection of  $\text{Cu}^{2+}$  ions in HepG2 cells. Images of bright field and fluorescence microscopy revealed that **1** and **2** treated cells did not show significantly detectable changes when compared to normal untreated control (Fig. 15a and 16a). But in cell sets of **1** and **2** treated with  $\text{Cu}^{2+}$ , the cells were found to be red in coloration when observed under bright field (Fig. 15c and 16c). The images also clearly suggest that the receptors are not only permeable through cell membrane (cytoplasm was red in colour) but also receptor effectively cross the nuclear membrane (nucleus were also red in colour). The effect was greater for **2** +  $\text{Cu}^{2+}$  than that of **1** +  $\text{Cu}^{2+}$ . However, no such changes were observed in fluorescent filter (Fig. 15d). On the other hand, cell sets incubated with either **2** +  $\text{Cd}^{2+}$ , **2** +  $\text{Zn}^{2+}$  and **2** +  $\text{Hg}^{2+}$  although showed no significant changes in bright field imaging (Fig. 16e, g and i) but a significant increase in fluorescent intensity in red filter was observed in the following order: **2** +  $\text{Cd}^{2+}$  < **2** +  $\text{Zn}^{2+}$  < **2** +  $\text{Hg}^{2+}$  when compared to untreated control cell set (Fig. 16f, h and j).

This suggests that both the receptors **1** and **2** are permeable through cellular membrane and can assist in sensing the presence of  $\text{Cu}^{2+}$ , even in a small concentration, in living tissues without imparting any significant cellular cytotoxicity. Even the receptor **2** in addition, is also able to detect the intercellular metal ions such as  $\text{Cd}^{2+}$ ,  $\text{Zn}^{2+}$  and  $\text{Hg}^{2+}$  ions effectively by exhibiting marked change in fluorescence.

Results of % cell viability assay suggest that the receptors **1** or **2** have no significant cellular cytotoxicity in HepG2 cells when compared to solvent treated cells (ESI, Fig. 24S†).

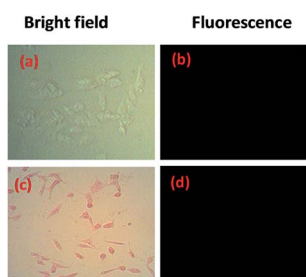


Fig. 15 Fluorescence and bright field images of HepG2 cells: (a) bright field image of cells treated with receptor **1** (10  $\mu\text{M}$ ) for 25 min at 25  $^{\circ}\text{C}$ , (b) fluorescence image of cells treated with **1** (10  $\mu\text{M}$ ) for 25 min at 37  $^{\circ}\text{C}$ , (c) bright field image of cells upon treatment with receptor **1** (10  $\mu\text{M}$ ) followed by  $\text{Cu}(\text{ClO}_4)_2$  (15  $\mu\text{M}$ ) for 1 h at 25  $^{\circ}\text{C}$ , (d) fluorescence image of cells upon treatment with **1** (10  $\mu\text{M}$ ) followed by  $\text{Cu}(\text{ClO}_4)_2$  (15  $\mu\text{M}$ ) for 1 h at 37  $^{\circ}\text{C}$  [red filter is used,  $\lambda_{\text{ex}} = 480\text{--}580\text{ nm}$ ].

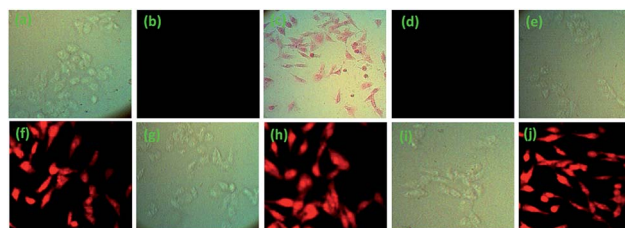


Fig. 16 Fluorescence and bright field images of HepG2 cells: (a) bright field image of cells treated with **2** (10  $\mu\text{M}$ ) for 25 min at 25  $^{\circ}\text{C}$ , (b) fluorescence image of cells treated with **2** (10  $\mu\text{M}$ ) for 25 min at 25  $^{\circ}\text{C}$ , (c) bright field image of cells upon treatment with **2** (10  $\mu\text{M}$ ) followed by  $\text{Cu}(\text{ClO}_4)_2$  (15  $\mu\text{M}$ ) for 1 h at 25  $^{\circ}\text{C}$ , (d) fluorescence image of cells upon treatment with **2** (10  $\mu\text{M}$ ) followed by  $\text{Cu}(\text{ClO}_4)_2$  (15  $\mu\text{M}$ ) for 1 h at 25  $^{\circ}\text{C}$ , (e) bright field image of cells upon treatment with **2** (10  $\mu\text{M}$ ) followed by  $\text{Cd}(\text{ClO}_4)_2$  (15  $\mu\text{M}$ ) for 1 h at 25  $^{\circ}\text{C}$ , (f) fluorescence image of cells upon treatment with **2** (10  $\mu\text{M}$ ) followed by  $\text{Cd}(\text{ClO}_4)_2$  (15  $\mu\text{M}$ ) for 1 h at 25  $^{\circ}\text{C}$ , (g) bright field image of cells upon treatment with receptor **2** (10  $\mu\text{M}$ ) followed by  $\text{Zn}(\text{ClO}_4)_2$  (15  $\mu\text{M}$ ) for 1 h at 25  $^{\circ}\text{C}$ , (h) fluorescence image of cells upon treatment with **2** (10  $\mu\text{M}$ ) followed by  $\text{Zn}(\text{ClO}_4)_2$  (15  $\mu\text{M}$ ) for 1 h at 25  $^{\circ}\text{C}$ , (i) bright field image of cells upon treatment with **2** (10  $\mu\text{M}$ ) followed by  $\text{Hg}(\text{ClO}_4)_2$  (15  $\mu\text{M}$ ) for 1 h at 25  $^{\circ}\text{C}$ , (j) fluorescence image of cells upon treatment with **2** (10  $\mu\text{M}$ ) followed by  $\text{Hg}(\text{ClO}_4)_2$  (15  $\mu\text{M}$ ) for 1 h at 25  $^{\circ}\text{C}$  [red filter is used in fluorescence imaging,  $\lambda_{\text{ex}} = 480\text{--}580\text{ nm}$ ].

## Conclusions

In conclusion, a new dipicolylamine coupled rhodamine B molecular sensor **1** has been designed and synthesized. The new sensor **1** displayed strong selectivity for  $\text{Cu}^{2+}$  ion over a series of other metal ions examined in  $\text{CH}_3\text{CN}/\text{aqueous Tris-HCl}$  buffer (4/1, v/v) at pH 7.2 by exhibiting a colour change (from colourless to pink). The sensor **1** has been detected to be insensitive to proton-induced-spirolactam ring opening in the pH range 4 to 12 and thus offers a large pH window for detection of metal ions. The ensemble of  $\mathbf{1}\cdot\text{Cu}^{2+}$  has further been successfully used for naked eye detection of  $\text{CN}^-$  ion over a series of other anions examined in the study. Thus the present finding offers a new example of dipicolyl amine (DPA)-based rhodamine molecule for  $\text{Cu}^{2+}$  ion in addition to the existing few examples for other metal ions such as  $\text{Zn}^{2+}$ ,  $\text{Al}^{3+}$  and  $\text{Pb}^{2+}$  in the literature.<sup>6,7</sup> The role of DPA motif in **1** for selective binding of  $\text{Cu}^{2+}$  ion has been established by considering the model compound **3**.

On the other hand, replacement of anthracene by butyl chain in receptor **2** shows that the receptor is able to detect  $\text{Cu}^{2+}$  colorimetrically and  $\text{Cd}^{2+}$ ,  $\text{Zn}^{2+}$  and  $\text{Hg}^{2+}$  ions fluorometrically. Like the case of **1**, the ensemble  $\mathbf{2}\cdot\text{Cu}^{2+}$  is also sensible to  $\text{CN}^-$  ion. Furthermore, the compounds **1** and **2** are cell permeable and can detect the intercellular mentioned metal ions through imaging process.

## Experimental

### Syntheses

#### 1-(Anthracen-9-yl)-N-(pyridin-2-ylmethyl)methanamine (**4**).

To a solution of 9-anthranaldehyde (1 g, 4.85 mmol) in dry

methanol, 2-picolyamine (0.519 g, 4.85 mmol) was added and the reaction mixture was refluxed for 6 h. The Schiff base 3, formed *in situ*, was reduced by refluxing the mixture with NaBH<sub>4</sub> (0.600 g, 15.86 mmol) for 6 h. The progress of the reduction was monitored by thin layer chromatography (TLC) (petroleum ether–EtOAc, 1 : 1, v/v). After completion of the reaction, the solvent was evaporated under reduced pressure. Then, CHCl<sub>3</sub>–water (2 : 1, v/v) was added to the residue and the compound was extracted with CHCl<sub>3</sub>. The organic phase was dried over anhydrous Na<sub>2</sub>SO<sub>4</sub> and evaporated *in vacuo*. The crude product was purified by column-chromatography using petroleum ether–EtOAc (1 : 1; v/v) as eluent to afford the amine 4 as a yellow gum (1.1 g, yield: 75.8%); <sup>1</sup>H NMR (400 MHz, CDCl<sub>3</sub>): δ 8.59 (d, 1H, *J* = 8 Hz), 8.39 (s, 1H), 8.31 (d, 2H, *J* = 8 Hz), 7.99 (d, 2H, *J* = 8 Hz), 7.68–7.64 (td, 1H, *J*<sub>1</sub> = 8 Hz, *J*<sub>2</sub> = 4 Hz), 7.53–7.43 (m, 4H), 7.38 (d, 1H, *J* = 8 Hz), 7.20–7.17 (m, 1H), 4.76 (s, 2H), 4.16 (s, 2H), 2.16 (br s, 1H, NH); FTIR (KBr, cm<sup>-1</sup>): 3411, 3050, 2856, 1589, 1432.

***N*-(6-(((Anthracen-9-ylmethyl) (pyridin-2-ylmethyl)amino) methyl)pyridin-2-yl)pivalamide (5).** To a stirred solution of amine 4 (0.400 g, 1.34 mmol) in 20 mL dry CH<sub>3</sub>CN, anhydrous K<sub>2</sub>CO<sub>3</sub> (0.300 g, 2.17 mmol) was added and the mixture was stirred for 30 min. Then 2-pivaloylamide-6-bromomethyl pyridine (0.363 g, 1.34 mmol) was added and the reaction mixture was refluxed for 6 h and the progress of the reaction was monitored by TLC. After completion of the reaction CH<sub>3</sub>CN was evaporated in a vacuum. CHCl<sub>3</sub>–water (3 : 1, v/v) was added to the residue and the compound was extracted with CHCl<sub>3</sub>. The combined organic layer was dried over anhydrous Na<sub>2</sub>SO<sub>4</sub> and the solvent was evaporated *in vacuo*. The crude product was purified through column chromatography using 35% EtOAc in petroleum ether as eluent to give 5 as a yellow solid (0.475 g, yield: 72.5%), mp 160 °C; <sup>1</sup>H NMR (400 MHz, CDCl<sub>3</sub>): δ 8.49 (d, 1H, *J* = 4 Hz), 8.39 (d, 2H, *J* = 8 Hz), 8.35 (s, 1H), 8.03 (d, 1H, *J* = 8 Hz), 7.95 (d, 2H, *J* = 8 Hz), 7.58–7.55 (m, 2H), 7.48–7.43 (m, 5H), 7.32 (d, 1H, *J* = 8 Hz), 7.12 (m, 1H), 7.01 (d, 1H, *J* = 8 Hz), 4.66 (s, 2H), 3.89 (s, 2H), 3.75 (s, 2H), 1.66 (s, 9H); FTIR (KBr, cm<sup>-1</sup>): 3417, 2959, 2832, 1689, 1449.

**6-(((Anthracen-9-ylmethyl)(benzyl)amino)methyl)pyridin-2-amine (6).** Compound 5 (0.400 mg, 0.81 mmol), taken in a 50 mL round-bottomed flask, was mixed with 4(N) KOH solution (4 mL) and ethanol (4 mL). The reaction mixture was then refluxed for 12 h. The completion of the reaction was monitored by TLC. Ethanol was distilled out and the product was extracted with ethyl acetate and dried over anhydrous sodium sulfate. Organic layer was evaporated to afford the compound 6 as yellow solid (0.250 g, yield: 75.7%), mp 186 °C. This was pure enough for the next step and for spectral analysis. <sup>1</sup>H NMR (400 MHz, CDCl<sub>3</sub>): δ 8.46–8.40 (m, 3H), 8.35 (s, 1H), 7.95 (d, 2H, *J* = 8 Hz), 7.58 (t, 1H, *J* = 8 Hz), 7.47–7.41 (m, 4H), 7.39–7.34 (m, 2H), 7.10–7.07 (m, 1H), 6.75 (d, 1H, *J* = 8 Hz), 6.34 (d, 1H, *J* = 8 Hz), 4.64 (s, 2H), 4.39 (s, 2H), 3.86 (s, 2H), 3.71 (s, 2H); <sup>13</sup>C NMR (100 MHz, CDCl<sub>3</sub>): δ 158.0, 157.7, 148.5, 138.0, 136.1, 131.5, 131.3, 130.0, 128.8, 127.5, 125.4, 125.2, 125.0, 124.7, 123.5, 121.8, 113.6, 106.6, 60.6, 60.5, 50.8; FTIR (KBr, cm<sup>-1</sup>): 3471, 3310, 2922, 1617, 1458.

***N*-(Pyridin-2-ylmethyl)butan-1-amine (8).** To a solution of pyridine-2-aldehyde (0.500 g, 4.67 mmol) in dry MeOH, *n*-butyl amine (0.512 mL, 7.00 mmol) was added and the reaction mixture was allowed to reflux for 6 h. The Schiff base 7 formed *in situ* was reduced by refluxing the mixture with NaBH<sub>4</sub> (0.317 g, 8.40 mmol) for 4 h. The reaction was quenched by evaporation of the solvent under reduced pressure. CHCl<sub>3</sub>–water (2 : 1) was added to the residue and extracted with CHCl<sub>3</sub>. The organic phase was dried over anhydrous Na<sub>2</sub>SO<sub>4</sub> and evaporated *in vacuo*. The crude product was purified by column-chromatography using petroleum ether/EtOAc, 10 : 1 (v/v) as eluent to afford the amine 8 as yellow liquid (0.650 g, yield: 84.8%), <sup>1</sup>H NMR (400 MHz, CDCl<sub>3</sub>): δ 8.36 (d, 1H, *J* = 4.4 Hz), 7.47–7.42 (m, 1H), 7.11 (d, 1H, *J* = 8 Hz), 6.97 (t, 1H, *J* = 6.2 Hz), 3.70 (s, 2H), 2.46 (t, 2H, *J* = 7.2 Hz), 1.92 (brs, 1H), 1.36–1.29 (m, 2H), 1.21–1.12 (m, 2H), 0.71 (t, 3H, *J* = 7.4 Hz). FTIR (KBr, cm<sup>-1</sup>): 3389, 2928, 1591, 1570.

***N*-(6-((Butyl(pyridin-2-ylmethyl)amino)methyl)pyridin-2-yl) pivalamide (9).** To a stirred solution of amine 8 (0.600 g, 3.64 mmol) in 25 mL dry CH<sub>3</sub>CN, anhydrous K<sub>2</sub>CO<sub>3</sub> (0.757 g, 5.48 mmol) was added and the mixture was stirred for 30 min. Then 2-pivaloylamide-6-bromomethyl pyridine (0.990 g, 3.65 mmol) was added and the reaction mixture was refluxed for 6 h and the progress of the reaction was monitored by TLC. After completion of the reaction, CH<sub>3</sub>CN was evaporated in vacuum. CHCl<sub>3</sub>–water (3 : 1, v/v) was added to the residue and the compound was extracted with CHCl<sub>3</sub>. The combined organic layer was dried over anhydrous Na<sub>2</sub>SO<sub>4</sub> and the solvent was evaporated *in vacuo*. The crude product was purified through column chromatography using 25% EtOAc in petroleum ether as eluent to give 9 as yellow gum (0.900 g, yield: 69.5%), <sup>1</sup>H NMR (400 MHz, CDCl<sub>3</sub>): δ 8.44 (d, 1H, *J* = 4.4 Hz), 8.01 (d, 1H, *J* = 8 Hz), 7.95 (s, 1H), 7.60–7.55 (m, 2H), 7.45 (d, 1H, *J* = 8 Hz), 7.19 (d, 1H, *J* = 8 Hz), 7.06 (t, 1H, *J* = 8 Hz), 3.72 (s, 2H), 3.61 (s, 2H), 2.44 (t, 2H, *J* = 8 Hz), 1.46–1.43 (m, 2H), 1.25 (s, 9H), 1.23–1.17 (m, 2H), 0.78 (t, 3H, *J* = 8 Hz); <sup>13</sup>C NMR (100 MHz, CDCl<sub>3</sub>): δ 177.0, 160.0, 158.4, 150.8, 148.8, 138.6, 136.3, 122.7, 121.8, 118.5, 111.8, 60.4, 60.0, 54.2, 39.7, 29.2, 27.4, 20.4, 13.9; FTIR (KBr, cm<sup>-1</sup>): 3437, 2958, 1690, 1596.

**6-((Butyl(pyridin-2-ylmethyl)amino)methyl)pyridin-2-amine (10).** Compound 9 (0.650 mg, 1.83 mmol), taken in a 50 mL round-bottomed flask, was mixed with 4(N) KOH solution (8 mL) and ethanol (8 mL). The reaction mixture was then refluxed for 4 h. The completion of the reaction was monitored by TLC. Ethanol was distilled out and the product was extracted with ethyl acetate and dried over anhydrous Na<sub>2</sub>SO<sub>4</sub>. Organic layer was evaporated to afford the compound 10 as yellow liquid (0.330 g, yield: 66.56%). This was used directly in the next step without characterization.

***N*-(3-Nitrobenzyl)butan-1-amine (12).** Compound 12 was obtained as yellow liquid (1.6 g, yield: 77.4%) from 3-nitrobenzaldehyde (1.5 g, 9.93 mmol) and *n*-butylamine (0.680 mL, 9.93 mmol) according to the procedure followed for the synthesis of 4. However, in this case, the intermediate Schiff base 11 was prepared in dry benzene. <sup>1</sup>H NMR (400 MHz, CDCl<sub>3</sub>): δ 8.13 (s, 1H), 8.02 (d, 1H, *J* = 8 Hz), 7.61 (d, 1H, *J* = 8

Hz), 7.41 (t, 1H,  $J = 8$  Hz), 3.82 (s, 2H), 2.55 (t, 2H,  $J = 8$  Hz), 2.09 (s, 1H), 1.46–1.39 (m, 2H), 1.33–1.26 (m, 2H), 0.84 (t, 3H,  $J = 8$  Hz); FTIR (KBr,  $\text{cm}^{-1}$ ): 3411, 3050, 2856, 1589, 1432.

**N-Benzyl-N-(3-nitrobenzyl)butan-1-amine (13).** Compound **13** was obtained as yellow liquid (1.0 g, yield: 69.8%) from amine **12** (1.0 g, 4.80 mmol) and benzyl bromide (0.830 mL, 4.80 mmol) according to the procedure followed for the synthesis of **5**.  $^1\text{H}$  NMR (400 MHz,  $\text{CDCl}_3$ ):  $\delta$  8.14 (s, 1H), 7.98 (d, 1H,  $J = 8$  Hz), 7.61 (d, 1H,  $J = 8$  Hz), 7.37 (t, 1H,  $J = 8$  Hz), 7.28–7.21 (m, 4H), 7.16–7.13 (m, 1H), 3.53 (s, 2H), 3.49 (s, 2H), 2.35 (t, 2H,  $J = 8$  Hz), 1.46–1.38 (m, 2H), 1.24–1.17 (m, 2H), 0.73 (t, 3H,  $J = 8$  Hz);  $^{13}\text{C}$  NMR (100 MHz,  $\text{CDCl}_3$ ):  $\delta$  148.3, 142.6, 139.4, 134.7, 129.0, 128.7, 128.3, 127.0, 123.4, 121.9, 58.4, 57.5, 53.4, 29.2, 20.4, 14.0; FTIR (KBr,  $\text{cm}^{-1}$ ): 2956, 2930, 1528, 1506, 1348.

**3-((Benzyl(butyl)amino)methyl)aniline (14).** To a stirred solution of **13** (0.700 g, 2.35 mmol) in 15 mL EtOH,  $\text{SnCl}_2$  (1.78 g, 9.38 mmol) was added and the reaction mixture was refluxed for 3 h and the progress of the reaction was monitored by TLC. After completion of the reaction, EtOH was evaporated maximally in vacuum. Then the reaction mixture was basified with aq.  $\text{NaHCO}_3$  solution and the organic compound was extracted with ethyl acetate (20 mL  $\times$  3). The organic layer was dried over anhydrous  $\text{Na}_2\text{SO}_4$  and the solvent was evaporated *in vacuo*. The crude product was purified through column chromatography using 10% EtOAc in petroleum ether as eluent to give amine **14** as gummy product (0.430 g, yield: 68.2%).  $^1\text{H}$  NMR (400 MHz,  $\text{CDCl}_3$ ):  $\delta$  7.28 (d, 2H,  $J = 8$  Hz), 7.23 (t, 2H,  $J = 8$  Hz), 7.15–7.11 (m, 1H), 7.01–6.97 (m, 1H), 6.69–6.65 (m, 2H), 6.46 (dd, 1H,  $J_1 = 8$  Hz,  $J_2 = 2.4$  Hz), 3.46 (s, 2H), 3.38 (s, 2H), 2.32 (t, 2H,  $J = 4$  Hz), 1.44–1.37 (m, 2H), 1.25–1.16 (m, 2H), 0.75 (t, 3H,  $J = 8$  Hz) (signal for  $-\text{NH}_2$  is not found due to broadening);  $^{13}\text{C}$  NMR (100 MHz,  $\text{CDCl}_3$ ):  $\delta$  146.3, 141.3, 140.0, 129.0, 128.8, 128.1, 126.6, 119.2, 115.4, 113.6, 58.2, 53.1, 29.2, 20.5, 14.1 (one carbon in the aliphatic region is unresolved); FTIR (KBr,  $\text{cm}^{-1}$ ): 3747, 2954, 2929, 1619, 1492.

**Receptor 1.** A solution of rhodamine B base (0.300 g, 0.62 mmol) in 1,2-dichloroethane (12 mL) was stirred, and phosphorus oxychloride (0.145 mL, 1.57 mmol) was added dropwise over 2 min. The solution was refluxed for 3 h. The reaction mixture was cooled and evaporated *in vacuo* to give rhodamine B acid chloride **15**, which was not purified and used in the next step directly. The crude acid chloride **15** was dissolved in dry  $\text{CH}_2\text{Cl}_2$  (25 mL) and was added to a solution of **6** (0.240 g, 0.59 mmol) in  $\text{CH}_2\text{Cl}_2$  (15 mL) containing  $\text{Et}_3\text{N}$  (0.263 mL). The reaction mixture was stirred at room temperature for 3 h. After completion of reaction, solvent was evaporated under reduced pressure. The crude product was purified by column chromatography using 35% EtOAc in petroleum ether as eluent to give receptor **1** as a yellow solid (0.290 g, yield: 55.9%), mp 110 °C;  $^1\text{H}$  NMR (400 MHz,  $\text{CDCl}_3$ ):  $\delta$  8.42 (d, 1H,  $J = 8$  Hz), 8.36 (d, 1H,  $J = 8$  Hz), 8.31 (s, 1H), 8.09 (d, 2H,  $J = 8$  Hz), 7.98 (d, 1H,  $J = 8$  Hz), 7.92 (d, 2H,  $J = 8$  Hz), 7.56 (t, 1H,  $J = 8$  Hz), 7.46–7.36 (m, 7H), 7.10 (d, 1H,  $J = 8$  Hz), 6.99–6.95 (m, 2H), 6.79 (d, 1H,  $J = 8$  Hz), 6.43 (d, 2H,  $J = 8$  Hz), 6.32 (d, 2H,  $J = 4$  Hz), 5.94 (d, 1H,  $J = 4$  Hz), 5.92 (d, 1H,  $J = 4$  Hz), 4.18 (s, 2H), 3.57 (s, 2H), 3.50 (s, 2H), 2.95–2.82 (m, 8H), 0.85 (t, 12H,  $J = 4$  Hz);  $^{13}\text{C}$  NMR (100 MHz,  $\text{CDCl}_3$ ):  $\delta$  168.6, 160.5, 156.7, 154.1, 153.1, 149.5, 148.2, 148.0, 137.0, 136.0, 133.5, 131.4, 131.3, 130.6, 129.9, 128.7, 127.9, 127.4, 127.1, 125.3, 125.2,

124.6, 124.3, 123.4, 123.1, 121.6, 119.5, 113.9, 108.6, 107.0, 97.7, 66.2, 59.9, 59.8, 50.1, 43.8, 12.4; FTIR (KBr,  $\text{cm}^{-1}$ ): 3385, 3049, 2965, 1700, 1614, 1514; HRMS (TOF MS  $\text{ES}^+$ ): calcd for  $(\text{M} + \text{H})^+$ : 829.4230, found:  $(\text{M} + \text{H})^+$ : 829.4265.

**Receptor 2.** The rhodamine acid chloride **15** was dissolved in dry  $\text{CH}_2\text{Cl}_2$  (35 mL) and was added to a solution of **10** (0.292 g, 1.08 mmol) in  $\text{CH}_2\text{Cl}_2$  (20 mL) containing  $\text{Et}_3\text{N}$  (0.376 mL, 2.71 mmol). The reaction mixture was stirred at room temperature for 6 h. After completion of reaction, solvent was evaporated under reduced pressure. The crude product was purified by column chromatography using 25% EtOAc in petroleum ether as eluent to give receptor **2** as pale pink solid (0.520 g, yield: 69.1%), mp 155 °C;  $^1\text{H}$  NMR (400 MHz,  $\text{CDCl}_3$ ):  $\delta$  8.48 (d, 1H,  $J = 4$  Hz), 8.31 (d, 1H,  $J = 8$  Hz), 8.00 (d, 1H,  $J = 8$  Hz), 7.57–7.47 (m, 4H), 7.33 (d, 1H,  $J = 8$  Hz), 7.16 (d, 1H,  $J = 8$  Hz), 7.10–7.04 (m, 2H), 6.43–6.38 (m, 4H, one doublet and one singlet are overlapped), 6.11 (dd, 2H,  $J_1 = 8$  Hz,  $J_2 = 2.4$  Hz), 3.61 (s, 2H), 3.47 (s, 2H), 3.32–3.22 (m, 8H), 2.30 (t, 2H,  $J = 8$  Hz), 1.34–1.28 (m, 2H), 1.18–1.10 (m, 14H), 0.73 (t, 3H,  $J = 8$  Hz);  $^{13}\text{C}$  NMR (100 MHz,  $\text{CDCl}_3$ ):  $\delta$  168.1, 153.7, 153.6, 149.4, 148.6, 148.2, 137.0, 136.2, 133.4, 130.6, 128.0, 127.7, 124.4, 123.0, 122.8, 121.6, 117.6, 113.1, 108.8, 106.9, 97.6, 66.2, 61.0, 59.9, 54.4, 44.2, 29.4, 20.3, 13.9, 12.6 (two carbons in the aromatic regions are unresolved); FTIR (KBr,  $\text{cm}^{-1}$ ): 3393, 3077, 2934, 1704, 1634, 1615; HRMS (TOF MS  $\text{ES}^+$ ): calcd for  $(\text{M} + \text{H})^+$ : 695.4073, found:  $(\text{M} + \text{H})^+$ : 695.4073.

**Receptor 3.** The rhodamine acid chloride **15** was dissolved in dry  $\text{CH}_2\text{Cl}_2$  (35 mL) and was added to a solution of **14** (0.300 g, 1.08 mmol) in  $\text{CH}_2\text{Cl}_2$  (20 mL) containing  $\text{Et}_3\text{N}$  (0.376 mL, 2.71 mmol). The reaction mixture was stirred at room temperature for 6 h. After completion of reaction, solvent was evaporated under reduced pressure. The crude product was purified by column chromatography using 10% EtOAc in petroleum ether as eluent to give the receptor **3** as colourless gum (0.340 g, yield: 72.5%);  $^1\text{H}$  NMR (400 MHz,  $\text{CDCl}_3$ ):  $\delta$  7.95–7.92 (m, 1H), 7.42 (t, 2H,  $J = 8$  Hz), 7.17–7.15 (m, 5H), 7.13–7.07 (m, 2H), 7.01 (t, 2H,  $J = 8$  Hz), 6.68 (s, 1H), 6.59 (d, 1H,  $J = 8$  Hz), 6.56 (d, 1H,  $J = 8$  Hz), 6.20 (dd, 2H,  $J_1 = 8$  Hz,  $J_2 = 2.4$  Hz), 6.13 (d, 2H,  $J = 2.4$  Hz), 3.26 (s, 2H), 3.24 (s, 2H), 3.21–3.14 (m, 8H), 2.13 (t, 2H,  $J = 8$  Hz), 1.30–1.26 (m, 2H), 1.18–1.09 (m, 2H), 1.03 (t, 12H,  $J = 8$  Hz), 0.71 (t, 3H,  $J = 4$  Hz);  $^{13}\text{C}$  NMR (100 MHz,  $\text{CDCl}_3$ ):  $\delta$  167.6, 153.2, 153.1, 148.6, 139.9, 136.3, 132.7, 131.1, 128.89, 128.86, 128.2, 128.0, 127.9, 127.2, 126.5, 125.5, 124.0, 123.3, 108.0, 106.4, 97.7, 66.3, 57.9, 57.7, 52.6, 44.2, 29.7, 20.3, 14.0, 12.5 (two carbons in the aromatic regions are unresolved); FTIR (KBr,  $\text{cm}^{-1}$ ): 3367, 2965, 2925, 1700, 1615; HRMS (TOF MS  $\text{ES}^+$ ): calcd for  $(\text{M} + \text{H})^+$ : 693.4169, found:  $(\text{M} + \text{H})^+$ : 693.4130.

### X-ray diffraction

Data sets were collected with a Nonius KappaCCD diffractometer. Programs used: data collection, COLLECT (R. W. W. Hooft, Bruker AXS, 2008, Delft, The Netherlands); data reduction Denzo-SMN;<sup>18</sup> absorption correction, Denzo;<sup>19</sup> structure solution SHELXS-97;<sup>20</sup> structure refinement SHELXL-97 (ref. 21) and graphics, XP (BrukerAXS, 2000). Thermals ellipsoids are shown with 30% probability,  $R$ -values are given for observed reflections, and  $wR^2$  values are given for all reflections.

**Exceptions and special features.** A badly disordered half benzene molecule was found in the asymmetrical unit and could not be satisfactorily refined. The program SQUEEZE<sup>22</sup> was therefore used to remove mathematically the effect of the solvent. The quoted formula and derived parameters are not included the squeezed solvent molecule.

### Computational details

Full geometrical optimizations of all the structures were carried out in the gas phase employing the Becke three-parameter hybrid density functional combined with the Lee–Yang–Parr correlation functional (B3LYP).<sup>23–26</sup> The DFT (B3LYP) calculations was performed with the 6-31G(d) basis set<sup>27</sup> for carbon, hydrogen, nitrogen and oxygen atoms and for the copper atom SDD basis set<sup>28</sup> was used. Frequency calculations were performed at the same level of theory to confirm that each stationary point was a local minimum (with zero imaginary frequency). All DFT calculations were performed with the Gaussian 09 suite of programs.<sup>29</sup>

### Material and methods for cell culture

**Reagents.** The reagents used in our study were of analytical grade and were procured from Sigma Aldrich, USA.

**Cell culture.** Human liver cancer cells (HepG2) were procured from National Centre for Cell Science, Pune, India.  $5 \times 10^5$  cells per mL were cultured in DMEM which was supplemented with 10% fetal bovine serum and 1% PSN antibiotic at 37 °C and 5% CO<sub>2</sub> supply.

**% cellular cytotoxicity.** Cellular cytotoxicity of **1** and **2** were assessed by following the standard protocol of Mossam,<sup>30</sup> where cells were plated in 96-well microplates for 24 hours along with either of **1** and **2** at different concentrations. At the end of incubation period MTT was added in each well and incubated for 4 h and then DMSO was further added for dissolving the formazan crystal. The absorbance was then measured at 595 nm in a microplate reader (Thermo scientific, Multiskan ELISA, USA).

**Bright field and fluorescence microscopy.** The cells were seeded and harvested at  $10^7$  cells per plate and grown to 70% confluency for microscopic imaging. Untreated control set of HepG2 cells served as the standard to detect any changes brought about by addition of **1** and **2**.<sup>31</sup> The other set of cells include the following: (i) **1**, (ii) **1** + Cu<sup>2+</sup>, (iii) **2**, (iv) **2** + Cu<sup>2+</sup>, (v) **2** + Cd<sup>2+</sup>, (vi) **2** + Zn<sup>2+</sup>, (vii) **2** + Hg<sup>2+</sup>. In each case 40 μl of either of **1** and **2** were added and incubated for 25 min and then they were further incubated with either of 40 μl of Cu<sup>2+</sup>/Cd<sup>2+</sup>/Zn<sup>2+</sup>/Hg<sup>2+</sup> and kept for 30 min. Images were then captured in bright field and fluorescence filter fitted microscope (Leica, Germany).

## Acknowledgements

We thank DST and UGC, New Delhi, Govt. of India for providing facilities in the university under SAP program. DT thanks CSIR, New Delhi, India for a fellowship.

## References

- (a) H. Tapiero, D. M. Townsend and K. D. Tew, *Biomed. Pharmacother.*, 2003, **57**, 386; (b) M. C. Linder and M. Hazegh-Azam, *Am. J. Clin. Nutr.*, 1996, **63**, 797; (c) R. Uauy, M. Olivares and M. Gonzalez, *Am. J. Clin. Nutr.*, 1998, **67**, 952; (d) R. A. Lovstad, *BioMetals*, 2004, **17**, 111.
- (a) E. L. Que, D. W. Domaille and C. J. Chang, *Chem. Rev.*, 2008, **108**, 1517; (b) G. L. Millhauser, *Acc. Chem. Res.*, 2004, **37**, 79; (c) G. Multhaup, A. Schlicksupp, L. Hess, D. Beher, T. Ruppert, C. L. Masters and K. Beyreuther, *Science*, 1996, **271**, 1406; (d) F. Tisato, C. Marzano, M. Porchia, M. Pellei and C. Santini, *Med. Res. Rev.*, 2010, **30**, 708.
- (a) J. W. Lee, H. S. Jung, P. S. Kwon, J. W. Kim, R. A. Bartsch, Y. Kim, S. J. Kim and J. S. Kim, *Org. Lett.*, 2008, **10**, 3801; (b) H. J. Kim, Y. S. Park, S. Yoon and J. S. Kim, *Tetrahedron*, 2008, **64**, 1294; (c) S. Kaur and S. Kumar, *Chem. Commun.*, 2002, 2840; (d) S. M. Park, M. H. Kim, J.-I. Choe, K. T. No and S. K. Chang, *J. Org. Chem.*, 2007, **72**, 3550; (e) Y. Xiang, A. Tong, P. Jin and Y. Ju, *Org. Lett.*, 2006, **8**, 2863; (f) H. S. Jung, M. Park, D. Y. Han, E. Kim, C. Lee, S. Ham and J. S. Kim, *Org. Lett.*, 2009, **11**, 3378; (g) S. H. Kim, J. S. Kim, S. M. Park and S. K. Chang, *Org. Lett.*, 2006, **8**, 371; (h) X. Qi, E. J. Jun, L. Xu, S. J. Kim, J. S. J. Hong, Y. J. Yoon and J. Yoon, *J. Org. Chem.*, 2006, **71**, 2881; (i) H. S. Jung, P. S. Kwon, J. W. Lee, J. I. Kim, C. S. Hong, J. W. Kim, S. Yan, J. Y. Lee, J. H. Lee, T. Joo and S. J. Kim, *J. Am. Chem. Soc.*, 2009, **131**, 2008; (j) K. Ghosh and T. Sen, *Beilstein J. Org. Chem.*, 2010, **6**, 44, DOI: 10.3762/bjoc.6.44; (k) T. Gunnlaugsson, J. P. Leonard and N. S. Murray, *Org. Lett.*, 2004, **6**, 1557; (l) K. M. K. Swamy, S. K. Ko, S. K. Kwon, H. N. Lee, C. Mao, J. M. Kim, K. H. Lee, J. Kim, I. Shin and J. Yoon, *Chem. Commun.*, 2008, 5915; (m) S. Goswami, D. Sen and N. K. Das, *Org. Lett.*, 2010, **12**, 856; (n) Z. Xu, J. Pan, D. R. Spring, J. Cui and J. Yoon, *Tetrahedron*, 2010, **66**, 1678; (o) H. Li, Y. Zhu, B. Shi, W. Qu, Y. Zhang, Q. Lin, H. Yao and T. Wei, *Supramol. Chem.*, 2015, **27**, 471; (p) G. C. Yu, Z. B. Zhang, C. Y. Han, M. Xue, Q. Zhou and F. H. Huang, *Chem. Commun.*, 2012, 2958; (q) X. F. Ji, Y. Yao, J. Y. Li, X. Z. Yan and F. H. Huang, *J. Am. Chem. Soc.*, 2013, **135**, 74277; (r) P. Wang, X. Z. Yan and F. H. Huang, *Chem. Commun.*, 2014, 5017; (s) Z. Hu, J. Hu, Y. Cui, G. Wang, X. Zhang, K. Uvdal and H. Gao, *J. Mater. Chem. B*, 2014, **2**, 4467.
- (a) K. Ghosh, T. Sarkar, A. Samadder and A. R. Khuda-Bukhsh, *New J. Chem.*, 2012, **36**, 2121; (b) G. He, X. Zhang, C. He, X. Zhao and C. Duan, *Tetrahedron*, 2010, **66**, 9762; (c) L. Yuan, W. Lin, B. Chen and Y. Xie, *Org. Lett.*, 2012, **14**, 432; (d) M. Kumar, N. Kumar, V. Bhalla, P. R. Sharma and T. Kaur, *Org. Lett.*, 2012, **14**, 406; (e) C. Kaewtong, J. Noisepphum, Y. Uppa, N. Morakot, N. Morakot, B. Wannoo, T. Tuntulanic and B. Pulpoka, *New J. Chem.*, 2010, **34**, 1104; (f) D. Maity, D. Karthigeyan, T. K. Kundu and T. Govindaraju, *Sens. Actuators, B*, 2013, **176**, 831; (g) C. Kar, M. D. Adhikari, A. Ramesh and G. Das, *Inorg. Chem.*, 2013, **52**, 743; (h) M. Kaur and D. H. Choi, *Sens.*

- Actuators, B*, 2014, **190**, 542; (i) S. Goswami, D. Sen, A. K. Das, N. K. Das, K. Aich, H. K. Fun, C. K. Quah, A. K. Maity and P. Saha, *Sens. Actuators, B*, 2013, **183**, 518; (j) M. Wang, F. Yan, Y. Zou, L. Chen, N. Yang and X. Zhou, *Sens. Actuators, B*, 2014, **192**, 512; (k) X. Zenga, L. Donga, C. Wua, L. Mua, S. F. Xuea and Z. Taa, *Sens. Actuators, B*, 2009, **141**, 506; (l) X. Zhang, Y. Shiraishi and T. Hirai, *Org. Lett.*, 2007, **9**, 5039.
- 5 (a) X. Chen, T. Pradhan, F. Wang, J. S. Kim and J. Yoon, *Chem. Rev.*, 2012, **112**, 1910 and references cited therein; (b) Y. Yang, Q. Zhao, W. Feng and F. Li, *Chem. Rev.*, 2013, **113**, 192.
- 6 (a) P. W. Du and S. J. Lippard, *Inorg. Chem.*, 2010, **49**, 10753; (b) E. Tomat and S. J. Lippard, *Inorg. Chem.*, 2010, **49**, 9113; (c) Y. Chen, Y. Bai, Z. Han, W. He and Z. Guo, *Chem. Soc. Rev.*, 2015, **44**, 4517; (d) L. Zhu, Z. Yuan, J. T. Simmons and K. Sreenath, *RSC Adv.*, 2014, **4**, 20398; (e) E. M. Nolan and S. J. Lippard, *Acc. Chem. Res.*, 2009, **42**, 193; (f) L. Zhu, A. H. Younes, Z. Yuan and R. J. Clark, *J. Photochem. Photobiol., A*, 2015, **311**, 1; (g) J. T. Simmons, Z. Yuan, K. L. Daykin, B. T. Nguyen, R. J. Clark, M. Shatruk and L. Zhou, *Supramol. Chem.*, 2014, **26**, 214; (h) Z. Yuan, A. H. Younes, J. R. Allen, M. W. Davidson and L. Zhu, *J. Org. Chem.*, 2015, **80**, 5600; (i) K. Sreenath, Z. Yuan, J. R. Allen, M. W. Davidson and L. Zhu, *Chem.-Eur. J.*, 2015, **21**, 867.
- 7 (a) X. He, N. Zhu and V. W. W. Yam, *Organometallics*, 2009, **28**, 3621; (b) X. Bao, Q. Cao, Y. Xu, Y. Gao, Y. Xu, X. Nie, B. Zhou, T. Pang and J. Zhu, *Bioorg. Med. Chem.*, 2015, **23**, 694; (c) J. Y. Kwon, Y. J. Jang, Y. J. Lee, K. M. Kim, M. S. Seo, W. Nam and J. Yoon, *J. Am. Chem. Soc.*, 2005, **127**, 10107.
- 8 S. Goswami, R. Mukherjee and J. Ray, *Org. Lett.*, 2005, **7**, 1283.
- 9 X-ray crystal structure analysis of **1**: formula  $C_{55}H_{52}N_6O_2$ ,  $M = 829.03$ , pale yellow crystal,  $0.12 \times 0.10 \times 0.08$  mm,  $a = 11.9474(2)$ ,  $b = 12.2845(3)$ ,  $c = 16.6972(5)$  Å,  $\alpha = 101.213(1)$ ,  $\beta = 90.250(1)$ ,  $\gamma = 98.643(1)^\circ$ ,  $V = 2375.1(1)$  Å<sup>3</sup>,  $\rho_{\text{calc}} = 1.159$  g cm<sup>-3</sup>,  $\mu = 0.071$  mm<sup>-1</sup>, empirical absorption correction ( $0.991 \leq T \leq 0.994$ ),  $Z = 2$ , triclinic, space group  $P\bar{1}$  (no. 2),  $\lambda = 0.71073$  Å,  $T = 223(2)$  K,  $\omega$  and  $\varphi$  scans, 21481 reflections collected ( $\pm h, \pm k, \pm l$ ),  $[(\sin \theta)/\lambda] = 0.59$  Å<sup>-1</sup>, 8200 independent ( $R_{\text{int}} = 0.063$ ) and 4915 observed reflections [ $I > 2\sigma(I)$ ], 572 refined parameters,  $R = 0.086$ ,  $wR^2 = 0.224$ , max. (min.) residual electron density 0.21 (−0.20) e Å<sup>-3</sup>, hydrogen atoms were calculated and refined as riding atoms ESI.†
- 10 P. Job, *Ann. Chim.*, 1928, **9**, 113.
- 11 P. T. Chou, G. R. Wu, C. Y. Wei, C. C. Cheng, C. P. Chang and F. T. Hung, *J. Phys. Chem. B*, 2000, **104**, 7818.
- 12 A. Caballero, R. Martinez, V. Lloveras, I. Ratera, J. Vidal-Gancedo, K. Wurst, A. Tarraga, P. Molina and J. Vaciana, *J. Am. Chem. Soc.*, 2005, **127**, 15666.
- 13 M. H. Lim, B. A. Wong, W. H. Pitcock Jr, D. Mokshagundam, M. H. Baik and S. J. Lippard, *J. Am. Chem. Soc.*, 2006, **128**, 14364.
- 14 (a) S. Dalapati, S. Jana, M. A. Alam and N. Guchhait, *Sens. Actuators, B*, 2011, **60**, 1106; (b) A. Rai, N. Kumari, R. Nair, K. Singh and L. Mishra, *RSC Adv.*, 2015, **5**, 14382; (c) Y. L. Duan, Y. G. Shi, J. H. Chen, X. H. Wu, G. K. Wang, Y. Zhou and J. F. Zhang, *Tetrahedron Lett.*, 2012, **53**, 6544; (d) G. Li, F. Taa, H. Wang, Y. Li and L. Wang, *Sens. Actuators, B*, 2015, **211**, 325.
- 15 S. L. Shen, X. F. Zhang, S. Y. Bai, J. Y. Miao and B. X. Zhao, *RSC Adv.*, 2015, **5**, 13341.
- 16 (a) A. P. De Silva, T. S. Moody and G. D. Wright, *Analyst*, 2009, **134**, 2385; (b) A. J. Moro, P. J. Cywinski, S. Korstena and G. J. Mohrac, *Chem. Commun.*, 2010, 1085; (c) S. Y. Kim and J. I. Hong, *Tetrahedron Lett.*, 2009, **50**, 2822; (d) B. Roy, A. S. Rao and K. H. Ahn, *Org. Biomol. Chem.*, 2011, **9**, 7774.
- 17 (a) X. Zhang, Y. Shiraishi and T. Hirai, *Tetrahedron Lett.*, 2007, **48**, 5455; (b) K. Sreenath, R. J. Clark and L. Zhu, *J. Org. Chem.*, 2012, **77**, 8268; (c) Z. Xu, J. Pan, D. R. Spring, J. Cui and J. Yoon, *Tetrahedron*, 2010, **66**, 1678.
- 18 Z. Otwinowski and W. Minor, *Methods Enzymol.*, 1997, **276**, 307.
- 19 Z. Otwinowski, D. Borek, W. Majewski and W. Minor, *Acta Crystallogr., Sect. A: Found. Crystallogr.*, 2003, **59**, 228.
- 20 G. M. Sheldrick, *Acta Crystallogr., Sect. A: Found. Crystallogr.*, 1990, **46**, 467.
- 21 G. M. Sheldrick, *Acta Crystallogr., Sect. A: Found. Crystallogr.*, 2008, **64**, 112.
- 22 A. L. Spek, *J. Appl. Crystallogr.*, 2003, **36**, 7.
- 23 A. D. Becke, *J. Chem. Phys.*, 1993, **98**, 5648.
- 24 C. Lee, W. Yang and R. G. Parr, *Phys. Rev. B: Condens. Matter Mater. Phys.*, 1988, **37**, 785.
- 25 B. Miehlich, A. Savin, H. Stoll and H. Preuss, *Chem. Phys. Lett.*, 1989, **157**, 200.
- 26 P. J. Stephens, F. J. Devlin, C. F. Chabalowski and M. J. Frisch, *J. Phys. Chem.*, 1994, **98**, 11623.
- 27 M. M. Francl, W. J. Pietro, W. J. Hehre, J. S. Binkley, M. S. Gordon, D. J. Defrees and J. A. Pople, *J. Chem. Phys.*, 1982, **77**, 3654.
- 28 D. Andrae, U. Haussermann, M. Dolg, H. Stoll and H. Preuss, *Theor. Chim. Acta*, 1990, **77**, 123.
- 29 M. J. Frisch, G. W. Trucks, H. B. Schlegel, G. E. Scuseria, M. A. Robb, J. R. Cheeseman, G. Scalmani, V. Barone, B. Mennucci, G. A. Petersson, H. Nakatsuji, M. Caricato, X. Li, H. P. Hratchian, A. F. Izmaylov, J. Bloino, G. Zheng, J. L. Sonnenberg, M. Hada, M. Ehara, K. Toyota, R. Fukuda, J. Hasegawa, M. Ishida, T. Nakajima, Y. Honda, O. Kitao, H. Nakai, T. Vreven, J. A. Montgomery Jr, J. E. Peralta, F. Ogliaro, M. Bearpark, J. J. Heyd, E. Brothers, K. N. Kudin, V. N. Staroverov, R. Kobayashi, J. Normand, K. Raghavachari, A. Rendell, J. C. Burant, S. S. Iyengar, J. Tomasi, M. Cossi, N. Rega, J. M. Millam, M. Klene, J. E. Knox, J. B. Cross, V. Bakken, C. Adamo, J. Jaramillo, R. Gomperts, R. E. Stratmann, O. Yazyev, A. J. Austin, R. Cammi, C. Pomelli, J. W. Ochterski, R. L. Martin, K. Morokuma, V. G. Zakrzewski, G. A. Voth, P. Salvador, J. J. Dannenberg, S. Dapprich, A. D. Daniels, O. Farkas, J. B. Foresman, J. V. Ortiz, J. Cioslowski and D. J. Fox, *Gaussian 09, Revision B01*, Gaussian, Inc., Wallingford CT, 2009.
- 30 T. Mossam, *J. Immunol. Methods*, 1983, **65**, 55.
- 31 A. Samadder, S. Das, J. Das and A. R. Khuda-Bukhsh, *Colloids Surf., B*, 2013, **109**, 10.